Contactless Palm Vein Recognition System with Integrated Learning Approach System

Ram Gopal Musunuru[1], Dr. T Sivaprakasam[2], Dr G Krishna Kishore[3]

Research Scholar, Department of Computer Science and Engineering,
Annamalai University, Annamalainagar, Tamilnadu, India[1]

Assistant Professor, Department of Computer Science and Engineering, Annamalai University,
Annamalainagar, Tamilnadu, India[2]

Professor, Department of CSE, Dhanekula Institute of Engineering and Technology, Vijayawada, Andhra Pradesh, India[3]

Abstract—**Palm Vein Recognition (PVR) is a new biometric authentication technology that provides both security and convenience. This paper describes a contactless PVR system (CPVR) that uses an integrated learning approach (ILA) to recognise the palm veins from the given input images while ensuring user comfort and ease of use. Contactless palm vein scanning technology is used in the proposed system, eliminating the need for physical contact with the scanning device. The proposed method combines advanced feature extraction techniques with a light gradient boosting machine (LightGBM) and transfer learning. A pre-trained model, EfficientNetB1, is used to train the model to extract significant factors from the input PVR images. The proposed method improves user comfort and reduces the risk of cross-contamination in environments where hygiene is critical, such as hospitals, banking, and other secured places. The cutting-edge contactless palm vein scanner captures the unique vein patterns beneath the user's palm without requiring direct physical contact. The proposed ILA illuminates and captures vein patterns using near-infrared (NIR) light, ensuring high accuracy and robustness. The system employs advanced pre-processing techniques and enhanced image segmentation techniques to continuously improve recognition accuracy. It adjusts to changes in the user's vein patterns over time, considering factors like ageing and injuries. The ILA improves the system's ability to adjust palm positioning and lighting changes. The ILA is also a Contactless Palm Vein Recognition System with numerous applications, such as access control, secure authentication for financial transactions, healthcare record access, and more. The system is built to be scalable, allowing organisations to use it in various settings, ranging from small-scale installations to large enterprise-level deployments. Finally, the proposed approach ILA used to recognise accurate users increased the detection rate.**

Keywords—Palm Vein Recognition (PVR); Light Gradient Boosting Machine (LightGBM); Transfer Learning; Integrated Learning Approach (ILA)

I. INTRODUCTION

A Contactless Palm Vein Recognition System (CPVR) is a form of biometric identification that identifies people based on the unique vein patterns in their palms. It is an intensely reliable and accurate authentication method that can be used for various applications such as access control, identity verification, and secure interactions. The system typically uses near-infrared (NIR) light to illuminate the palm's veins. Hemoglobin in the blood absorbs this light, creating a distinct pattern of dark lines (veins) against a brighter background. The reflected light is captured by a camera or sensor, which makes an image of the palm's vein pattern. Advanced algorithms are used to extract and encode the unique vein pattern as a biometric template from this image. Because it requires a living hand with blood flow to function, Palm Vein Recognition (PVR) is known for its accuracy and resistance to spoofing. There are several limitations over the 2D-PVR such as less authentication, mismatched results Etc. In CPVR the advanced technique that helps in providing the high security is full-view 3D finger vein verification technique [1]. This technique leverages the unique patterns of blood vessels within an individual's finger to verify their identity [2]. In biometrics and computer vision, learning significant and selective indicators for palm print feature extraction and identification is essential [3]. Palm print recognition is a biometric authentication technique that uses an individual's palm's unique patterns of lines, ridges, and wrinkles [4].

Collecting and organizing data from various sources, ensuring accuracy and diversity, and implementing a secure storage and access system are all part of creating an innovative multidimensional vein database with fingerprints from the palm dorsal and wrist [5]. CNNs are commonly used in computer vision tasks because they can learn hierarchical features from images automatically. Concatenation refers to the process of combining or stacking features learned at different layers of the network for further processing [6]. A semantic feature selector is a component that aids in the identification and selection of the most pertinent features from a concatenated set of features. This step is critical for reducing the dimensionality of the data and retaining only the most discriminative features for vein recognition [7]. The concatenated feature vector is subjected to a semantic feature selector or another machine learning algorithm. This selector aids in the identification of the most informative features while excluding less relevant ones [8]. It could employ techniques like feature importance scores or attention mechanisms. Based on the vein pattern, the system uses classification or similarity scores to authenticate or verify the individual's identity.

The auto-encoder is trained to reduce the reconstruction error between the input vein images and the decoder output. This procedure fine-tunes the encoder to extract relevant vein patterns while filtering out noise and irrelevant data [9]. To

learn a compact and meaningful representation of the vein images, a DenseNet-based auto-encoder is used. Because of their dense connections and feature reuse, DenseNet architectures have produced excellent results in image-processing tasks. The auto-encoder's encoder compresses the input images into a lower-dimensional latent space while preserving essential features. When an individual's identity is verified, their vein image is passed through the trained encoder, producing a feature vector. Then, between this feature vector and the feature vectors stored in the database, a similarity measure, such as cosine similarity or Euclidean distance, is computed [10]. The individual is verified as a legitimate user if the similarity score exceeds a predefined threshold.

II. LITERATURE SURVEY

Cho et al. [11] introduced a novel approach that identifies the palm vein and the palm-print obtained from the given input image in NIR spectral bands. The proposed novel approach focused on extracting the features of palm-vein and palm-print that enhances the model using the LBP approach. The scores gained by identifying the proposed and noticed techniques have shown. Finally, the scores show that the proposed approach received better results based on the checking performance. Xi et al. [12] introduced the parallel NN approach integrated with the texture features applied to facial expressions—the proposed approach developed by using the CNN, RBN, and capsule network. The components were extracted using GLCM and combined with features belonging to actual images. The accuracy reaches 98.16%, which is more improved up to 3.71% compared with existing models. Finally, the proposed approach provides a better solution for image classification.Putro et al. [13] introduced the CNN-based face detector with a tiny architecture. The proposed approach contains two types of features, unique and multimodal facial features that help predict the multiple variations. The training mainly improves the outcomes by managing the loss and twitch on training configuration. The proposed approach solves the wider face detection issues by integrating the training features with the proposed method. Finally, the proposed system executes the 53 frames per second by processing high-resolution videos. Vu et al. [14] proposed the fast palm ROI extraction technique to tackle the complex issues. The proposed approach follows the contactless platform by using the free hand posture that finds the problems and increases the accuracy for ROI. Finally, the proposed method obtained high accuracy based on the extraction of palm ROI. Wu et al. [15] proposed a sophisticated denoisingResNet model, which combines the wavelet denoising (WD) and squeeze-and-excitation ResNet18 (SER) approaches. Skin noise and optical discoloration were removed from palm vein images using the WD method. The WD approach uses residual learning technology to improve the tiny-frequency feature into the DL feature. Finally, the suggested approach had been verified via a series of investigations. Sun et al. [16] introduced the plan view detection algorithm based on NPE and KELM. The proposed approach is integrated with preprocessing, feature extraction, and dimensionality reduction based on classification and recognition. Finally, the results show better

performance compared with existing systems. Li et al. [17] introduced a novel prevention system called VeinGuard. The novel approach combines DL algorithms, designed using the local-GAN, which prevent adversarial palm-vein image attacks. This approach contains the input images from different attacks that show the malicious attacks and reduce the computation time. Finally, the proposed system offers better accuracy based on adversarial attacks. Qin et al. [18] introduced the SSPP called the PVI approach, which contains multi-stage and multi-direction AGAN. An advanced data augmentation is used to find the patches in one image. The proposed approach includes the total conv GAN layers that distribute the input in different directions and detect the PVI. The proposed shows the accuracy, which is high compared with existing approaches. Yang et al. [19] introduced the low-rank initialization that extracts significant data from finger vein images. Various image-based fluctuations weaken the correlation among the original pictures and destroy the low-rank initialization. Finally, training aids in redesigning the low-rank coefficient to improve finger vein recognition performance. Qin et al. [20] introduced the iterative DBN that helps extract the vein features from the label data, and it is dynamically generated by using limited time to modify the DBN. The proposed system is integrated with several steps, like segmentation of input images by identifying the pixels of the image. The redesigned training model is used to predict the chances of the existing approach. The proposed method achieved accurate hand-vein recognition, showing better accuracy.Yang et al. [21] proposed a novel FV-GAN approach that solves various issues, such as extracting the accurate FV patterns with low-contrast IR finger images with less awareness. DL models such as CNN and others show a massive response on detection FV, but due to the more significant number of layers and size of the finger image, it takes more processing time. CNN has the drawback of showing less feature initialization because of low-quality FV image that contains eccentric and vessel breaks. To overcome all these issues, a novel approach, FV-GAN, offers high performance in reducing processing time. Das et al. [22] proposed the CNN-based FV identification system that analyzes the functionalities of the developed network from four publicly available networks. The proposed approach aims to provide constant and high accuracy when implemented with various qualities. The evaluation results show that the proposed CNN model obtained a high accuracy above 95.1%, which is high compared with existing models. Pan et al. [23] proposed the advanced DCNN approach that helps detect the Multi-Scale Deep Representation Aggregation (MSDRA) model using a pre-trained model DCNN to see finger veins. The proposed approach combines various techniques, such as detecting the multi-stage features with classification using SVM. The proposed method uses two datasets for the evaluation of results. Finally, the MSDRA shows better accuracy based on finger vein recognition.Song et al. [24] introduced the CNN model that contains two methods: difference image and measuring the distance among the feature vector obtained from the CNN. The difference between images is vulnerable to noise, and differences in pixel values create them. The proposed approach solves the issues developed by DenseNet, which shows massive performance in

terms of accuracy. To address issues with massive noise, Shen et al. [25] introduced a lightweight CNN model for finger vein image recognition and matching, obtaining the ROI and finger vein pattern feature. The proposed system solves the problems identified based on the lack of accuracy and more computation time. The proposed system received 99.4% and 99.45% accuracy, which is better than existing models. Hou et al. [26] proposed a new loss technique that learns the inter-class and intra-class data simultaneously by using the CNN for finger vein verification. Finally, the proposed approach obtained the efficiency and effectiveness of the proposed method. Kuzu et al. [27] introduced advanced finger vein pattern detection that captures accurate patterns using the CNN. The dataset is from videos with different times from 101 subjects. The proposed approach obtained an accuracy of 99.34%, better than existing approaches. Huang et al. [28] proposed the observation technique called joint attention that enables vigorous adaptation and data accumulation to extract the fine-grained details, which improves the finger vein patterns to obtain the identity features. The dimensionality reduction removes the feature maps and outcomes with highly significant features. Finally, the proposed approach, JAFVNet, shows effective performance in terms of accuracy. Yang et al. [29] developed a new biometric security system based on finger vein biometrics. The proposed BDD-ML-ELM looks at safeguarding the initial finger-vein structure even if its altered revision is affected; ultimately, the BDD-ML-ELM enhanced attack detection reliability over the current techniques. Yang et al. [30] presented the FVRAS-Net, a significant CNN approach using an MTL model to achieve high security and real-time performance. Finally, the proposed method achieves accuracy in terms of Finger-Vein Recognition rate.

III. METHODOLOGY

This section explains the methodology of this paper. The proposed approach is an integrated approach that recognizes the palm vein by using integrated learning approach (ILA). ILA contains various methods that help in fine tune the results for better outcomes. A pre-trained model EfficientNetB1is used as training model as a first step. Second, various preprocessing or noise filter approaches are used to remove the noise from input images. A feature extraction method feature-level fusion combined with several methods obtains the accurate features from the palm vein dataset. Finally the transfer learning is used to combine with LightGBM gives the accurate output for the development of Contactless Palm Vein Recognition System (CPVR) which is shown in Fig. 1. Fig. 1 also represents the methods that are used in this work.

A. Pre-trained Model for Contactless Palm Vein Recognition System (CPVR)

EfficientNet is a DL-based pre-trained model released in 2019. EfficientNetB1 is a neural network architecture developed in 2019 by Google researchers. These architectures are known for being efficient in terms of computational resources and model size, making them suitable for a wide range of computer vision tasks. The EfficientNet family is based on a concept known as compound scaling, which involves simultaneously scaling the network's depth, width, and resolution. It allows for a balance between model capacity

and computational cost. EfficientNetB1 is one of the models in this family, with fewer computational resources than more significant variants like B2, B3, and so on. To reduce computational complexity while maintaining representation power, it employs a variety of efficient building blocks, including depthwise separable convolutions. This paper employs the EfficientNetB1 as a pre-trained model and trains the Palm Vein using datasets such as polyu 2D images.

The following key factors of EfficientNetB1 are given below:

B. Width Scaling Factor (ϕ)

The width scaling factor, often denoted as phi (ϕ), determines the width of the network and affects the number of channels in each layer. It's typically chosen from a set of predefined values. For EfficientNetB1, ϕ is set to 1.0.

C. Depth Scaling Factor (α)

The depth scaling factor, alpha (α), determines the number of layers in the network. It's also chosen from a predefined set. For EfficientNetB1, alpha is set to 1.1.

D. Resolution Scaling Factor (Resolution)

The resolution scaling factor is used to adjust the input image resolution. Given that the base resolution is 224x224 for EfficientNetB1, you can calculate the new resolution using this formula:

$$\text{New Resoulution} = 224 * \text{resolution} \qquad (1)$$

where "resolution" is a value greater than 1, which increases the input resolution, or less than 1, which decreases it.

E. Number of Layers (N)

In ever block the no of layers of EfficientNetB1 can be calculated using the depth scaling factor alpha (α) as follows:

$$N = 1.33^{\propto} \qquad (2)$$

where $\propto$ represents exponentiation.

F. Number of Channels in Each Layer (C)

In ever block the no of layers of EfficientNetB1 can be calculated using the width scaling factor phi (ϕ) as follows:

$$C = 32 * \text{round}(\phi * 1.0) \qquad (3)$$

G. Number of Blocks in Each Stage (S)

The number of blocks in each stage is a design choice, and for EfficientNetB1, it typically consists of 4, 6, or 8 blocks in each stage. This value can vary depending on specific implementations.

H. Preprocessing Technique

Preprocessing is a critical step in removing noise from input PVR images. Noise removal is an important step in image processing that improves image quality by removing unwanted artifacts or distortions caused by various sources of noise. To reduce noise in the palm vein image, median filtering is used. Uneven illumination or sensor artifacts can both cause noise. The median filter is effective at removing salt-and-pepper noise, which causes some pixels to randomly

change to maximum or minimum values. It replaces each pixel with the median value of a specified neighborhood. Another method for removing noise is the Wavelet transform, which divides an image into multiple scales and allows for separate processing of different frequency components. Wavelet denoising techniques use threshold to remove noise while preserving image features. The Gabor Filter is also used to enhances the texture features can highlight the vein patterns.

The median filter for every input is represented as:

I. *Median Filter*

Let $I(a, b)$ initializes the actual image.

Let $I_{filtered}(a, b)$ represents the final output image.

1) Operation of median filter

- The median filter operation is carried out by dragging a window of a given size (MN) across the entire image.

- The median filter calculates the pixel values within the window centered at (a, b) for each pixel in the input image at coordinates (a, b).

- The corresponding pixel in the output (filtered) image at the exact coordinates (a,b) is then assigned the median value.

2) Median calculation: Sort the pixel values in the window in ascending order and choose the middle value to find the median value in a pixel's neighborhood. If the window size is even, the average of the two central values will be used. The median calculation for a 33 is as follows:

$$I_{filtered}(a, b) = median(I(a-1)(b-1), I(a, b-1), I(x+1, y-1), I(a-1, b), I(a, b), I(a), I(b) \qquad (4)$$
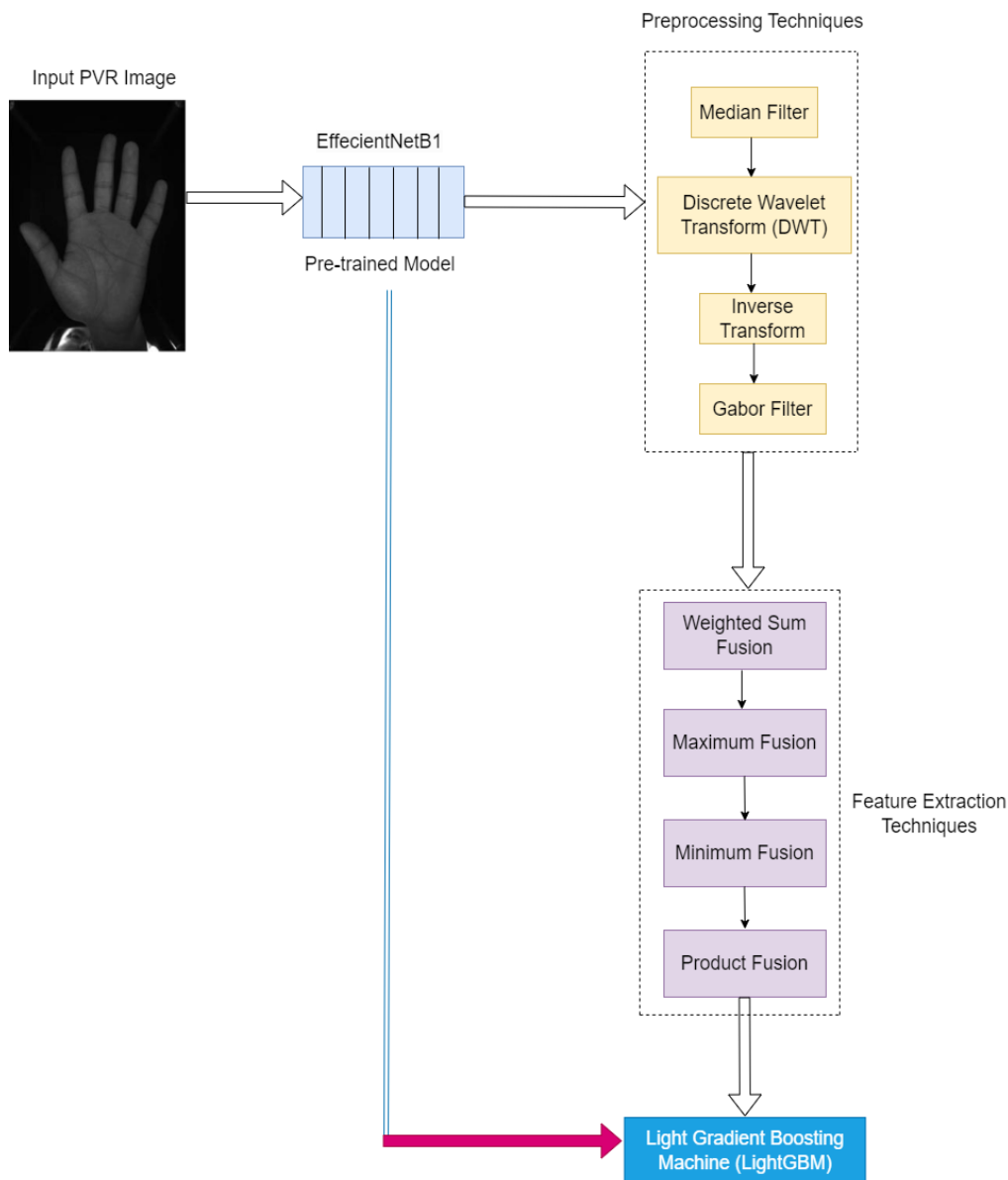
Fig. 1. Architecture diagram.

IV. DISCRETE WAVELET TRANSFORM (DWT)

The DWT is a mathematical technique for analyzing and decomposing two-dimensional images into various frequency components. A signal is divided into two parts in the DWT: approximation (low-frequency components) and detail (high-frequency components). A low-pass filter (LPF) and a high-pass filter (HPF) are used to achieve this decomposition. These filters are also known as analysis filters. The DWT equations are written as follows:

In the first step, the decomposition of input signals represented as $x[n]$:

Apply the LPF to achieve approximation coefficients (cX):

$$cX[j] = \sum_k x[k] * ho[k - 2j] \tag{5}$$

where, $h0[k]$ is the impulse response of the LPF.

Apply the HPF to achieve the detail coefficients (cY):

$$cY[j] = \sum_k x[k] * h1[k - 2j] \tag{6}$$

where, $h1[k]$ is the impulse response of the HPF.

Here, j represents the scale or level of the wavelet transform, and $cX[j]$ and $cY[j]$ are the estimation and specific coefficients at scale j, respectively.

A. Inverse Transform

The synthesis filters and formulas can reconstruct the actual signal from the estimation and specific coefficients. Synthesis filters are frequently the "dual" filters of analysis filters.

Apply the LPF to achieve approximation coefficients (cX) to get the approximation at the previous scale ($cX[j - 1]$):

$$cX[j - 1] = \sum_k cX[k] * g0[2(j - 1) - k] \tag{7}$$

where, $g0[j]$ is the impulse response of the syntheis LPF.

Apply the LPF to achieve approximation coefficients (cY) to get the approximation at the previous scale ($cY[j - 1]$):

$$cY[j - 1] = \sum_k cY[k] * g1[2(j - 1) - k] \tag{8}$$

where, $1[k]$ is the impulse response of the syntheis HPF.

Iteratively repeat these reconstruction steps, beginning with the finest scale (j = J) and ending with the coarsest scale (j = 1) until you obtain the reconstructed signal x[n].

B. Gabor Filter (GF)

It is one of the significant filters that used for tasks such as Palm Vein Recognition (PVR). These filters capture an image's texture and spatial frequency characteristics. Gabor filters can be used in Palm Vein Recognition to extract features unique to the palm veins. The equations and formulas for Gabor filters and their application in Palm Vein Recognition are as follows:

The 2D GF is defined as:

$$G(x, y; \lambda, \theta, \sigma, \gamma = \exp\left(-\frac{x'^2 + \gamma^2 y'^2}{2\sigma^2}\right) \cos\left(2\pi \frac{x'}{\lambda} + \theta\right) \tag{9}$$

where:

x and y are the coordinates of the pixel in the image.

λ is the wavelength of the sinusoidal component of the filter.

θ Represents inclination of the GF.

σ Represents standard deviation.

γ is the spatial ratio, controlling the ellipticity of the filter.

$x' = x\cos(\theta) + y\sin(\theta)$ and $y' = -x\sin(\theta) + y\cos(\theta)$ are the rotated coordinates.

C. Gabor Filter Bank:

A GF bank is created by varying the values of and capturing information at multiple scales and orientations. The filter responses for each parameter combination are computed for the input image.

V. FEATURE EXTRACTION TECHNIQUE FOR CPVR USING FEATURE-LEVEL FUSION

In Palm vein Recognition (PVR), feature-level fusion combines multiple palm vein features extracted from different sources or sensors to improve overall recognition accuracy. Various mathematical operations are used to achieve the fusion process. The following fusion methods used to extract the features from input images:

Weighted Sum Fusion: This method assigns weights to each feature source and combines them linearly.

$$\text{Fused Feature} = \sum(W_i * \text{Feature}_i) \tag{10}$$

Maximum Fusion: This method selects the maximum value for each feature dimension across all sources.

$$\text{FusedFeature}[j] = \max\left(\text{Feature}_{1[j]}, \text{Feature}_{2[j]}, \ldots, \text{Feature}_{N[j]}\right) \tag{11}$$

Minimum Fusion: Similar to Maximum Fusion, but it selects the minimum value for each feature dimension.

$$\text{FusedFeature}[j] = \min\left(\text{Feature}_{1[j]}, \text{Feature}_{2[j]}, \ldots, \text{Feature}_{N[j]}\right) \tag{12}$$

Product Fusion: This method multiplies the feature vectors element-wise from different sources.

$$\text{FusedFeature}[j] = \text{Feature}_{1[j]}, \text{Feature}_{2[j]}, \ldots, \text{Feature}_{N[j]} \tag{13}$$

where, N is the number of feature sources.

A. Light Gradient Boosting Machine (LightGBM) with Transfer Learning

LightGBM is a well-known gradient boosting framework that can be used for various machine learning tasks such as Palm Vein Recognition. LightGBM is a gradient-boosting framework that predicts using an ensemble of decision trees. It is intended to be fast, memory efficient, and scalable. In machine learning, transfer learning is typically defined as using knowledge gained from one task or dataset to improve performance on a related job or dataset. On the other hand, transfer learning is not commonly applied to gradient-boosting algorithms like LightGBM, which are primarily used for

tabular data and need a simple mechanism for incorporating knowledge from other domains or tasks. The following steps help to provide better outcomes for CPVR.

Step 1: Loss Function: For regression and classification tasks, LightGBM employs a variety of objective functions. During training, these functions are optimized.

$$\text{For Regression: } L(y, F) = \frac{1}{2} * \sum (y_i - F_i)^2 \quad (14)$$

Step 2: For binary classification, the logistic loss is commonly used

$$\text{For Regression: } L(y, p) = \sum \log(1 + e^{(-pi)}) + n(1 - y_i) * \log(1 + e^{pi})) \quad (15)$$

L is the loss function.

y is the true label.

F or p is the predicted output of the model.

Step 3: Gradient and Hessian Calculation

LightGBM computes the gradients and Hessians of the loss function concerning the predicted values. These gradients and Hessians determine the magnitude and direction of the model's parameter updates (trees). The gradients and Hessians are unique to the loss function.

Scalars function $f(x)$ where x is a vector of variables.

Gradient (∇f): The gradient of f is a vector that consists of partial derivatives of f with respect to every variable in x, it is initialized as $\frac{\partial f}{\partial x}$. Each component of the gradient is measured as follows:

$$\frac{\partial f}{\partial x_i} \quad (16)$$

where, x_i is the i-th variable in the vector x. Thus, the full gradient vector is:

$$\nabla f = \left[\frac{\partial f}{\partial x_1}, \frac{\partial f}{\partial x_2}, \ldots, \frac{\partial f}{\partial x_n}\right] \quad (17)$$

Hessian $(\nabla^2 f)$: The Hessian matrix is a matrix of squares containing the derivatives that are partial to f about each variable in x. It is denoted as $\frac{\partial^2 f}{\partial x^2}$. the elements of the Hessian matrix are computed as follows:

$$\frac{\partial^2 f}{\partial x_i \, \partial x_j} \quad (18)$$

where, x_i and x_j are variables in the vector x. So, the full Hessian matrix is an n×n matrix, where n is the number of variables, and its elements are computed for all combinations of i and j.

Step 4: Tree Building: LightGBM builds trees in a leaf-wise manner. The algorithm selects the leaf node that results in the maximum reduction in the loss function. The leaf-wise growth strategy is different from traditional depth-first or level-wise strategies used in other gradient boosting algorithms.

Step 5: Leaf Value Calculation: When a tree node is split, LightGBM calculates the value assigned to each leaf node. This calculation aims to optimize the loss function, taking into account the gradients and Hessians. The optimal leaf values are used to update the predictions.

Step 6: Shrinkage (Learning Rate): LightGBM typically uses a shrinkage parameter (learning rate) to control the step size of updates during the optimization process. This parameter prevents the model from making large adjustments in each iteration.

B. Dataset Description

The CASIA multi-spectral palm print image database was compiled from online sources and includes 3600 samples for training and 3600 samples for testing collected from 100 people [31]. Here six types of palm print images are shown in Fig. 2.
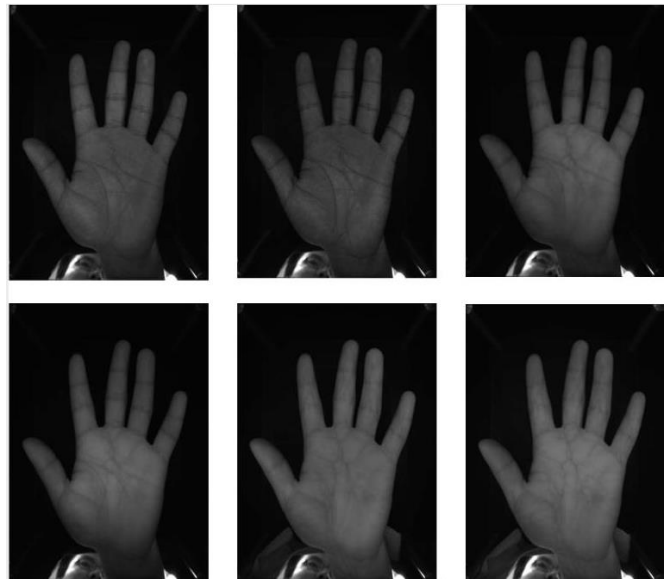
Fig. 2. Six types of palm vein images.

C. Performance Metrics

False Acceptance Rate (FAR): FAR calculates the likelihood of the system misidentifying an unauthorized user as authorized. A lower FAR denotes greater security.

$$FAR = \frac{\text{No of False Acceptances}}{\text{Total No of Identification Attempts}} \times 100\% \quad (19)$$

where:

"Number of False Acceptances" represents total no of incorrectly accepts an imposter.

"Total Number of Identification Attempts" is the total number of authentication or identification attempts, including both genuine and impostor attempts.

False Rejection Rate (FRR): The FRR calculates the likelihood of the system not accepting an authorized user. A lower FRR is preferable for user ease.

$$FRR = \frac{\text{No of False Rejections}}{\text{Total No of original Attempts}} \times 100\% \quad (20)$$

"Number of False Rejections" refers to the instances where the system incorrectly rejects a valid input or user.

"Total Number of Genuine Attempts" is the total number of times the system was presented with valid inputs or users.

Equal Error Rate (EER): The EER is a case where FAR and FRR are equivalent. Lower EER values suggest better system efficiency overall.

$$EER = \frac{(FAR+FRR)}{2} \qquad (21)$$

D. Experimental Results

This section focused on evaluation results of the LightBGM with transfer learning of PVRC. Python is powerful programming language that provides the better libraries to implement the proposed algorithm. An advanced hardware requirements like 32 GB RAM and I7 processor is needed to the system to execute the large PVR image dataset. The performance of pre-trained models such as EfficientNetB1 compared with several pre-trained models achieved the better results. The training and testing loss of EffecientNetB1 is explained in Fig. 3 and Fig. 4.

Fig. 3. The performance of EfficientNetB1 in terms of training and testing loss.
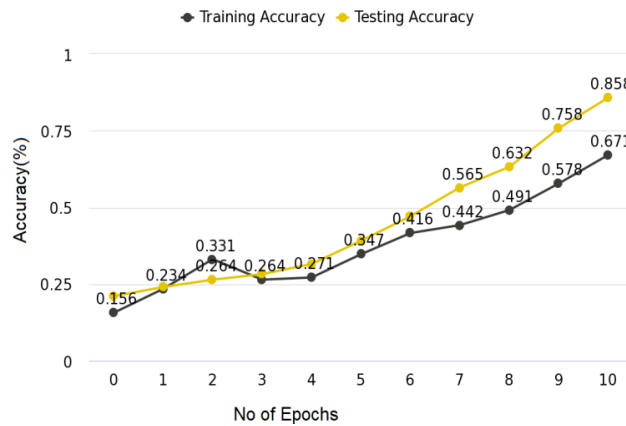
Fig. 4. The performance of EffecientNetB1 in terms of training and testing accuracy.

Fig. 3 shows the training and testing loss of EffecientB1 pre-trained model. Totally for 10 Epochs the loss is about 0.135% for 1st Epoch. There is Epoch iteration is starts from 10 Epoch to zeroEpoch. Here the training loss is low with 0.772% represents the lowest error rate. The training loss is about 0.743% which is low compare with testing loss and it prevents the over fitting. Fig. 4 shows the training and testing accuracy the training accuracy is about 0.671% and testing accuracy is about 0.858%.

Table I shows the comparative performance of various existing and proposed pre-trained models based on the FAR parameters. From the comparison it is shown that the proposed model shows the better outcomes compare with existing models. Table II shows the performance of several pre-trained models compared with the proposed model and obtained the outcomes based on the given parameter FRR. The FRR(%) shows very low compare with existing models that represents the better performance. Finally, these models help the proposed approach to show significant outcomes.

Table III shows the comparative outcomes of various pre-trained models for analyzing the performance in terms of ERR. Among all the models the proposed model shows the low error rate with high performance. Table IV shows the high performance in terms of all the parameters. Fig. 5 shows the overall performances of list of algorithms for CPVR.

TABLE I.   PERFORMANCE OF PRE-TRAINED MODELS IN TERMS OF FAR

Algorithms		Year	FAR (%)
MobileNet_v3	Howard et al.[32]	2019	7.56
GhostNet	Han et al.[33]	2020	6.78
RESNET	Zhang et al.[34]	2020	5.97
EffecientNetB1	Ours	-	4.54

TABLE II.   PERFORMANCE OF PRE-TRAINED MODELS IN TERMS OF FRR

Algorithms		Year	FRR (%)
MobileNet_v3	Howard et al.[32]	2019	6.23
GhostNet	Han et al.[33]	2020	5.23
RESNET	Zhang et al.[34]	2020	5.97
EffecientNetB1	Ours	-	3.76

TABLE III.   PERFORMANCE OF PRE-TRAINED MODELS IN TERMS OF ERR

Algorithms		Year	ERR (%)
MobileNet_v3	Howard et al.[32]	2019	6.895
GhostNet	Han et al.[33]	2020	6.55
RESNET	Zhang et al.[34]	2020	5.97
EffecientNetB1	Ours	-	4.15

TABLE IV. The Overall performances of list of Algorithms with Noise Filters

Algorithms		Year	EER (%)	FRR (%)	ERR (%)
PCANet with DL	Meraoumia et al.[35]	2021	0.949	1.789	1.567
CNN with Auto Encoder	Thapar et al. [36]	2017	3.71	2.987	2.123
CNN+ Bayesian Optimization + Jerman Filter	Obayya et al.[37]	2020	0.0683	0.0765	1.765
EffecientNetB1+ LightBGM with Transfer Learning	Ours	-	0.0541	0.0345	0.0235

	EER	FRR	ERR
PCANet with DL	0.949	1.789	1.567
CNN with Auto Encoder	3.71	2.987	2.123
CNN+ Bayesian Optimization + Jerman Filter	0.0683	0.0765	1.765
EffecientNetB1+ LightBGM with Transfer Learning	0.0541	0.0345	0.0235
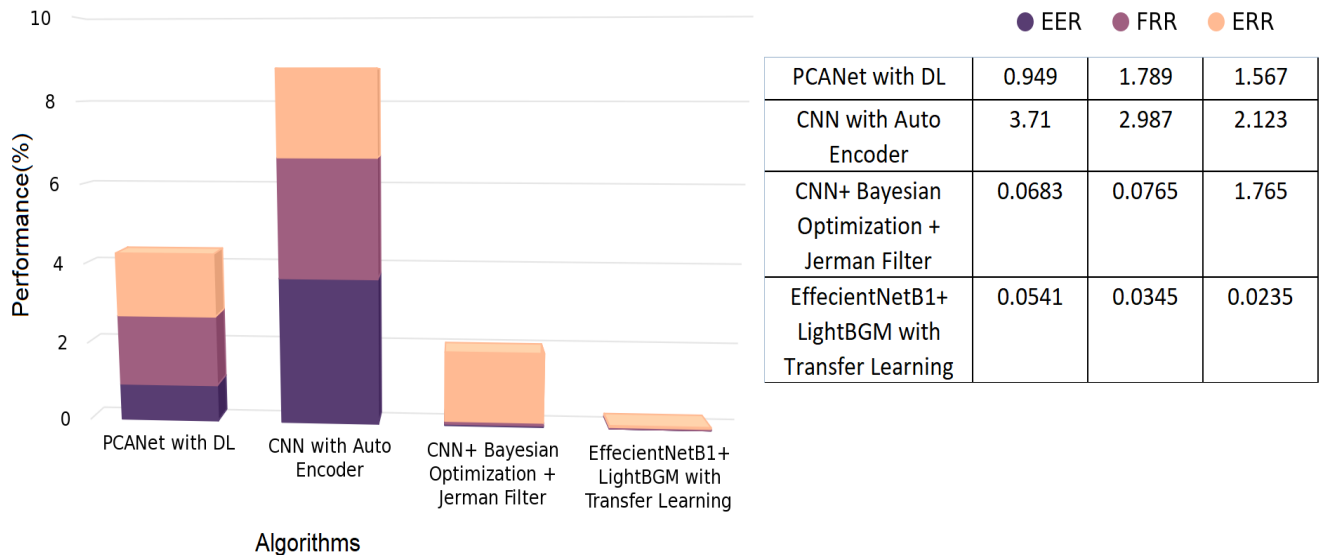
Fig. 5. The overall performances of list of algorithms for CPVR.

VI. CONCLUSION

The Integrated Learning Approach (ILA) for CPVR was introduced in this paper as a promising advancement in biometric security technology. Palm Vein Recognition is inherently secure because it relies on an individual's palm's unique vascular patterns. Contactless systems, in particular, reduce contamination risk while improving user convenience. The ILA combines several algorithms and methods to improve the system's accuracy and reliability. It ensures the system can produce consistent results even in various environmental conditions. Contactless systems are user-friendly and non-intrusive because they do not require physical contact. It can boost user acceptance and make the system suitable for various applications. Palm Vein Recognition is generally fast, allowing for quick and efficient access control or authentication. ILA improves this speed even further by optimizing the recognition process. Finally, ILA holds great promise in enhancing security, accuracy, and user experience across various applications. Its combination of contactless technology and advanced algorithms makes it an appealing option for businesses looking for dependable and secure biometric authentication solutions. However, as with any technology, factors such as implementation, user education, and ongoing maintenance must be considered to maximize the benefits of such systems while ensuring user privacy and data protection.

REFERENCES

[1] W. Kang, H. Liu, W. Luo and F. Deng, "Study of a full-view 3D finger vein verification technique", IEEE Trans. Inf. Forensics Security, vol. 15, pp. 1175-1189, 2019.

[2] B. Nakisa, F. Ansarizadeh, P. Oommen and S. Shrestha, "Technology Acceptance Model: A Case Study of Palm Vein Authentication Technology," in IEEE Access, vol. 10, pp. 120436-120449, 2022, doi: 10.1109/ACCESS.2022.3221413.

[3] S. Zhao and B. Zhang, "Learning salient and discriminative descriptor for palmprint feature extraction and identification", IEEE Trans. Neural Netw. Learn. Syst., vol. 31, no. 12, pp. 5219-5230, Dec. 2020.

[4] Wu, W., Elliott, S.J., Lin, S., Sun, S. and Tang, Y. (2020), Review of palm vein recognition. IET Biom., 9: 1-10.

[5] O. Toygar, F. O. Babalola and Y. Bitirim, "FYO: A novel multimodal vein database with palmar dorsal and wrist biometrics", IEEE Access, vol. 8, pp. 82461-82470, 2020.

[6] Z. Pan, J. Wang, Z. Shen, X. Chen and M. Li, "Multi-layer convolutional features concatenation with semantic feature selector for vein recognition", IEEE Access, vol. 7, pp. 90608-90619, 2019.

[7] G. Wang, C. Sun and A. Sowmya, "Multi-weighted co-occurrence descriptor encoding for vein recognition", IEEE Trans. Inf. Forensics Security, vol. 15, pp. 375-390, 2020.

[8] H. Qin, M. A. El Yacoubi, J. Lin and B. Liu, "An iterative deep neural network for hand-vein verification", IEEE Access, vol. 7, pp. 34823-34837, 2019.

[9] R. S. Kuzu, E. Maiorana and P. Campisi, "Vein-based biometric verification using densely-connected convolutional autoencoder", IEEE Signal Process. Lett., vol. 27, pp. 1869-1873, 2020.

[10] S. -J. Horng, D. -T. Vu, T. -V. Nguyen, W. Zhou and C. -T. Lin, "Recognizing Palm Vein in Smartphones Using RGB Images," in IEEE

Transactions on Industrial Informatics, vol. 18, no. 9, pp. 5992-6002, Sept. 2022, doi: 10.1109/TII.2021.3134016.

[11] S. Cho, B. Oh, K. Toh and Z. Lin, "Extraction and cross-matching of palm vein and palmprint from the RGB and the NIR spectrums for identity verification", IEEE Access, vol. 8, pp. 4005-4021, 2020.

[12] Z. Xi, Y. Niu, J. Chen, X. Kan and H. Liu, "Facial expression recognition of industrial internet of things by parallel neural networks combining texture feature", IEEE Trans. Ind. Informat., vol. 17, no. 4, pp. 2784-2793, Apr. 2021.

[13] M. D. Putro, L. Kurnianggoro and K.-H. Jo, "High performance and efficient real-time face detector on central processing unit based on convolutional neural network", IEEE Trans. Ind. Informat., vol. 17, no. 7, pp. 4449-4457, Jul. 2021.

[14] D.-T. Vu, T.-V. Nguyen and S.-J. Horng, "Rotation-invariant palm ROI extraction for contactless recognition" in Advances in Computer Vision and Computational Biology, Cham, Germany::Springer, pp. 701-715, 2021.

[15] [15] W. Wu et al., "Outside Box and Contactless Palm Vein Recognition Based on a Wavelet Denoising ResNet," in IEEE Access, vol. 9, pp. 82471-82484, 2021, doi: 10.1109/ACCESS.2021.3086811.

[16] S. Sun, X. Cong, P. Zhang, B. Sun and X. Guo, "Palm Vein Recognition Based on NPE and KELM," in IEEE Access, vol. 9, pp. 71778-71783, 2021, doi: 10.1109/ACCESS.2021.3079458.

[17] Y. Li, S. Ruan, H. Qin, S. Deng and M. A. El-Yacoubi, "Transformer Based Defense GAN Against Palm-Vein Adversarial Attacks," in IEEE Transactions on Information Forensics and Security, vol. 18, pp. 1509-1523, 2023, doi: 10.1109/TIFS.2023.3243782.

[18] H. Qin, M. A. El-Yacoubi, Y. Li and C. Liu, "Multi-scale and multi-direction GAN for CNN-based single palm-vein identification", IEEE Trans. Inf. Forensics Security, vol. 16, pp. 2652-2666, 2021.

[19] L. Yang, G. Yang, K. Wang, F. Hao and Y. Yin, "Finger vein recognition via sparse reconstruction error constrained low-rank representation", IEEE Trans. Inf. Forensics Security, vol. 16, pp. 4869-4881, 2021.

[20] H. Qin, M. A. E. Yacoubi, J. Lin and B. Liu, "An iterative deep neural network for hand-vein verification", IEEE Access, vol. 7, pp. 34823-34837, 2019.

[21] W. Yang, C. Hui, Z. Chen, J.-H. Xue and Q. Liao, "FV-GAN: Finger vein representation using generative adversarial networks", IEEE Trans. Inf. Forensics Security, vol. 14, no. 9, pp. 2512-2524, Sep. 2019.

[22] R. Das, E. Piciucco, E. Maiorana and P. Campisi, "Convolutional neural network for finger-vein-based biometric identification", IEEE Trans. Inf. Forensics Security, vol. 14, no. 2, pp. 360-373, Jun. 2019.

[23] Z. Pan, J. Wang, G. Wang and J. Zhu, "Multi-scale deep representation aggregation for vein recognition", IEEE Trans. Inf. Forensics Security, vol. 16, pp. 1-15, 2021.

[24] J. M. Song, W. Kim and K. R. Park, "Finger-vein recognition based on deep DenseNet using composite image", IEEE Access, vol. 7, pp. 66845-66863, 2019.

[25] J. Shen et al., "Finger vein recognition algorithm based on lightweight deep convolutional neural network", IEEE Trans. Instrum. Meas., vol. 71, pp. 1-13, 2022.

[26] B. Hou and R. Yan, "Arcvein-arccosine center loss for finger vein verification", IEEE Trans. Instrum. Meas., vol. 70, pp. 1-11, 2021.

[27] R. S. Kuzu, E. Piciucco, E. Maiorana and P. Campisi, "On-the-fly finger-vein-based biometric recognition using deep neural networks", IEEE Trans. Inf. Forensics Security, vol. 15, pp. 2641-2654, 2020.

[28] J. Huang, M. Tu, W. Yang and W. Kang, "Joint attention network for finger vein authentication", IEEE Trans. Instrum. Meas., vol. 70, pp. 1-11, 2021.

[29] W. Yang, S. Wang, J. Hu, G. Zheng, J. Yang and C. Valli, "Securing deep learning based edge finger vein biometrics with binary decision diagram", IEEE Trans. Ind. Informat., vol. 15, no. 7, pp. 4244-4253, Jul. 2019.

[30] W. Yang, W. Luo, W. Kang, Z. Huang and Q. Wu, "FVRAS-Net: An embedded finger-vein recognition and antispoofing system using a unified CNN", IEEE Trans. Instrum. Meas., vol. 69, no. 11, pp. 8690-8701, Nov. 2020.

[31] Ying Hao Zhenan Sun,Tieniu Tan and Chao Ren, "Multi-spectral palm image fusion for accurate contact-free palmprint recognition", Proceedings of IEEE International Conference on Image Processing, 2008, pp.281-284, USA

[32] A. Howard, M. Sandler, B. Chen. W. J. Wang, L. C. Chen, M. X. Tan, G. Chu, V. Vasudevan, Y. K. Zhu, R. M. Pang, H, Adam, Q. Le. Searching for mobileNetV3. In Proceedings of IEEE/CVF International Conference on Computer Vision, IEEE, Seoul, South Korea, pp.1314–1324, 2019. DOI: 10.1109/ICCV.2019.00140.

[33] K. Han, Y. H. Wang, Q. Tian, J. Y. Guo, C. J. Xu, C. Xu. GhostNet: More features from cheap operations. [Online], Available: https://arxiv.org/abs/1911.11907, 2019.

[34] H. Zhang, C. R. Wu, Z. Y. Zhang, Y. Zhu, Z. Zhang, H. B.Lin, Y. Sun, T. He, J. Mueller, R. Manmatha, M. Li, A.Smola. ResNeSt: Split-attention networks. [Online], Available: https://arxiv.org/abs/2004.08955, 2020.

[35] A. Meraoumia, F. Kadri, H. Bendjenna, S. Chitroub, and A. Bouridane, "Improving biometric identification performance using PCANet deep learning and multispectral palmprint," in Signal Processing for Security Technologies. Cham, Switzerland: Springer, 2017, pp. 51–69.

[36] D. Thapar, G. Jaswal, A. Nigam, and V. Kanhangad, "PVSNet: Palm vein authentication siamese network trained using triplet loss and adaptive hard mining by learning enforced domain specific features," in Proc. IEEE 5th Int. Conf. Identity, Secur., Behav. Anal. (ISBA), Jan. 2019, pp. 1–8, doi: 10.1109/ISBA.2019.8778623.

[37] M. I. Obayya, M. El-Ghandour and F. Alrowais, "Contactless Palm Vein Authentication Using Deep Learning With Bayesian Optimization," in IEEE Access, vol. 9, pp. 1940-1957, 2021, doi: 10.1109/ACCESS.2020.3045424.